CHAPTER FIVE

The Impact of Buildings on Urban Air Quality

Contents

Introduction 105
Primary Effects of Buildings on Dispersion of Traffic Emissions 108
- The Impact of Buildings on Mean Winds and Turbulence Within the Urban Canopy 110
- Vortex Flow and Street Canyons 112
- Challenges for Practical Application of Models of Building Effects on Dispersion 115
- Primary Variables Governing Dispersion in Cities 117

Models for the Effects of Buildings 119
- Operational Street Pollution Model 119
- Vertical Dispersion Model 121

Comparison of Model with Observations 124
- Description of the Los Angeles Field Measurements 125
- Evaluation of the VDM with Data Collected in Los Angeles and Riverside 127

Summary 133
References 135
Further Reading 136

INTRODUCTION

A major challenge facing air pollution regulators and researchers is the need to better characterize the factors that influence exposure to traffic emissions in cities. Early studies of exposure and health effects relied on estimates of exposure concentrations at a person's home location. However, studies that recorded a person's actual exposure using mobile personal exposure monitors that were carried by the subject showed that the personal exposure could be significantly higher than the exposure implied by the measured or modeled concentration at the person's home. These studies concluded that an individual's daily activities and the time spent within microenvironments associated with elevated concentrations

Urban Transportation and Air Pollution.
DOI: https://doi.org/10.1016/B978-0-12-811506-0.00005-1

are important factors that determine actual exposure. The exposure varies depending on the degree to which traffic sources influence the exposure concentrations within the person's home, work, school, and commute microenvironments. The subject of this chapter is the impact that the urban built environment has on exposure concentrations. Buildings tend to reduce dispersion and thus create hot spots associated with elevated concentrations of traffic emissions. In this chapter, we show practical methods to model these hot spot concentrations.

The need to employ accurate models of exposure to traffic emissions is driven by policies aimed at increasing high-density development within cities. These policies, which are meant to reduce greenhouse gas emissions from transportation, rely on reducing vehicle miles traveled to achieve desired reductions in fossil fuel consumption. To accomplish this, the policies incorporate plans for development that place high-density housing in close proximity to businesses and transportation infrastructure. These designs are often called sustainable communities or transit-oriented development (TOD) and are desirable because they promote walking, cycling, and use of public transportation, all of which reduce use of motor vehicles and the associated pollutant and greenhouse gas emissions. However, there is concern that these community designs create pollutant hot spots next to high-density built-up areas, which can reduce dispersion and thus magnify the concentrations of vehicle-emitted pollutants.

The impact of the presence of buildings near the road on dispersion of traffic emissions is manifested at multiple spatial scales ranging from the city scale to the scale of individual buildings. When viewed at the city scale, the effect of the buildings is to increase the surface roughness length and surface heat flux of the city relative to that produced by vegetation and natural terrain, and the resulting impact on mean winds and turbulence translates into modified dispersion relative to the flat terrain models presented in Chapter 3. The urban canopy refers to the region between the ground and the average height of urban buildings. The winds and turbulence within the urban canopy are dominated by the drag force of the buildings. At spatial scales on the order of the building height, individual buildings induce wake flows and recirculating vortices. The combination of these effects modifies the dispersion of traffic emissions with the result that concentrations are significantly different from those that would be observed in rural environments. This has significant implications for the design and

application of regulatory and research dispersion models for estimating the impact of roadways on exposure concentrations in cities.

Regulatory and research dispersion models account for the primary effects of buildings on dispersion using varying approximations, and the models can be classified according to the type of physical phenomena they describe and the spatial resolution they treat. The US EPA regulatory model AERMOD (Cimmorelli et al., 2005) incorporates the effects of buildings at the neighborhood and city scale. AERMOD uses the city population to estimate the enhanced positive heat flux and the increased boundary layer height due to convection that occurs in urban areas during nighttime. These boundary layer parameters are translated into increased turbulence and dispersion during nighttime in urban areas. AERMOD includes the PRIME algorithm that estimates plume downwash in building wakes. However, PRIME is designed for isolated point sources near single buildings and thus is not applicable to estimating the impact of buildings on dispersion of roadway emissions at the street scale.

Thus, in the United States, application of models of building effects at the street scale has been limited primarily to research use. Europe has seen more widespread use of these models for both research and operational applications such as routine air quality forecasting. The most well-known example of the operational models is the Operational Street Pollution Model (OSPM, Berkowicz et al., 1997), developed by the Danish National Environmental Research Institute. OSPM is a street canyon model; Street canyons are streets with tall buildings on either side, the building walls thus forming a canyon. The driving flow above the top of the buildings induces recirculating vortex flows within the canyon, leading to trapping of pollutants within the street. Street canyon models describe dispersion at the scale of individual streets and thus the spatial resolution of these models is 10−100 m. We will discuss more about street canyon models and OSPM in the next section.

In this chapter, we show how the primary effects of buildings on dispersion are incorporated into semiempirical models. The models discussed are useful for estimating the near-road concentration of traffic emissions in urban areas. We focus on the street scale, with an associated spatial resolution of 10−100 m, which is the scale at which roadways impact near-road environment. We begin by reviewing the relevant experimental and modeling studies and describing the physical effects of buildings on dispersion of traffic emissions. Next, we present the formulation of dispersion models that account for these effects. The model development focuses on two models:

OSPM and the Vertical Dispersion Model (VDM). OSPM is included because of its position as a well-known model that can be considered a prototype for the class of street canyon models that describe dispersion within the urban near-road environment. However, OSPM is primarily designed for European cities, whose streets tend to closely match the idealized street canyon model. Cities with nonuniform building heights and spatial inhomogeneity tend to have wind and turbulence patterns that are inconsistent with the street canyon model formulation. Additionally, it is difficult to define the model input parameters needed for street canyon models when the building geometry does not match the street canyon prototype. We make the case that VDM is useful for describing dispersion in spatially inhomogeneous cities with nonuniform building heights, such as those often found in urban cores in the United States. Finally, we describe the evaluation of VDM with observations.

PRIMARY EFFECTS OF BUILDINGS ON DISPERSION OF TRAFFIC EMISSIONS

This section reviews the primary effects of buildings on dispersion. The governing physical processes are active at different spatial or temporal scales, and thus models for these processes are built to match these scales. The effects of buildings occur at spatial scales including the street scale, 10−100 m, the neighborhood scale, 100 m−1 km, the urban background scale, 1−10 km, and the regional scale, 10−100 km. Models for the effects of buildings at each scale are combined in a hierarchy, with the smaller scales providing the most local detail and with these small-scale effects being parameterized using simplifications within the larger scale models. This chapter describes models of the near-road concentrations of traffic emissions, and thus this section focuses on effects that occur at the street scale. Chapter 6 reviews effects that occur at larger spatial scales and describes models of the impact of buildings on dispersion at these scales. We first give an overview of the important physics ranging from street to urban background scales to provide context for the present discussion.

Our discussion of the effects of buildings at different spatial scales is in part modeled on that provided by Britter and Hanna (2003). Fig. 5.1 shows a schematic of the effects of buildings after a transition from a rural area with low surface roughness length into the urban area. When viewed at the city

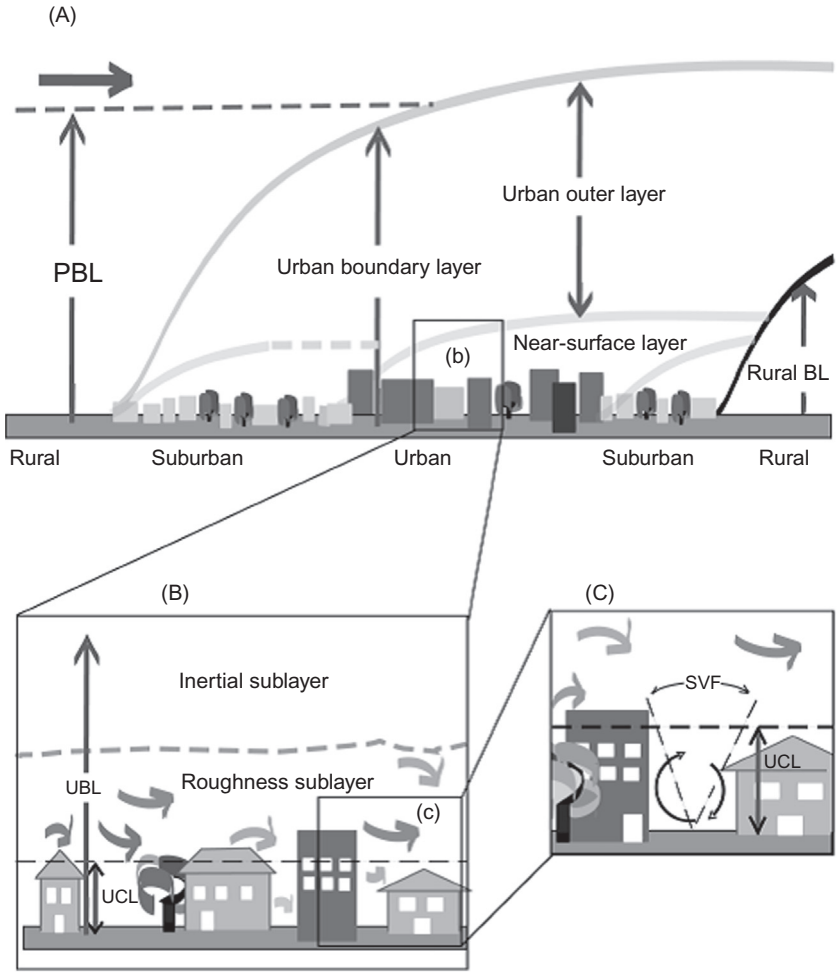

Figure 5.1 Schematic showing the effects of buildings at different spatial scales. Schematic is taken from Fisher et al. (2006). (A) Mesoscale; (B) local scale; and (C) microscale. PBL refers to the planetary boundary layer height.

scale, the impact of individual buildings on the flow and dispersion is averaged out and thus the buildings can be described using statistical parameters. At this scale, the primary impact of the built environment is through modifications of the drag force and the surface energy balance. As air flows from the upwind rural, low surface roughness area into the city, a region develops where the wind is modified due to the increased drag applied by the buildings. The zone where the wind speed is modified is the internal boundary layer (IBL). The height of the IBL grows with distance from the rural–urban

boundary. The wind that has adjusted to the urban surface roughness conditions is the urban boundary layer (UBL). The UBL can be divided into regions where different physical processes dominate. The near-surface UBL flow is described by the roughness sublayer and the inertial sublayer, similar to the way we describe flow over a rural surface. The roughness sublayer is the region, up to a few building heights from the ground, where the dominant length scale is the building height, and the flow is dominated by the effects of the building "roughness elements." Thus, the flow within the roughness sublayer is horizontally inhomogeneous. Above the roughness sublayer is the inertial sublayer, where the dominant length scale is the height from the ground, and similarity profiles can be used to model the wind, displaced upward by an amount proportional to the building height and with the surface roughness determined by building morphology. Models for these effects are described in more detail in Chapter 6. In this section, we focus on the region below the top of the buildings, called the urban canopy layer (UCL). This is the region where the physics of dispersion that governs the near-road concentration within an individual street is active. The UCL is the region described by street canyon dispersion models.

The effect of the buildings at scales larger than the street scale is usually parameterized using statistical measures of the building morphology. These measures typically include the average building height and measures of the building density, including the frontal and plan area fractions (Oke, 1988). The frontal area fraction, $\lambda_f = A_f/A_d$, is the ratio of the frontal area of the obstacles perpendicular to the mean wind direction, A_f, to the ground surface area occupied by the city, A_d. Thus, this parameter describes the building area upon which the drag force acts per unit area of the city. The plan area fraction is the fraction of ground surface area occupied by the buildings, $\lambda_p = A_p/A_d$, where A_p is the area of the buildings when viewed from the top. The area fractions are often used to describe the wind and turbulence within the UCL.

The Impact of Buildings on Mean Winds and Turbulence Within the Urban Canopy

The mean winds and turbulence within the UCL have several key characteristics that significantly influence the dispersion of traffic emissions. First, the mean wind speeds are small compared with winds in rural areas because of the drag force that the buildings exert on the air flow. Second, turbulence levels tend to be increased relative to those in the rural area. The result of the increased turbulence and low winds is that pollutant

plumes in urban areas exhibit significant horizontal meandering due to large, relative to the mean wind, lateral turbulent fluctuations. Finally, building wakes generate strong upward and downward flows as well as vortex flows. These flows form the basis of street canyon dispersion models. We begin by discussing the impact of the buildings on mean winds and turbulence within the urban canopy.

Mean winds and turbulence within the roughness sublayer and the urban canopy are usually described using statistical methods. Thus, while the flow around individual buildings is strongly influenced by the local building geometry, we can develop models to describe the horizontally averaged winds and turbulence within the roughness sublayer and the urban canopy. This horizontal averaging requires that the statistical parameters describing the buildings are horizontally homogeneous over the spatial averaging area. Thus, the city may be divided into regions where average values of the parameters such as the surface roughness length, building height, and area fractions can be assigned. The change in surface roughness of these regions is associated with the formation of an IBL and the adjustment of the wind and shear stress within and above the canopy to the new equilibrium values. For the assumption that the wind adjusts to the new surface conditions to be valid, the horizontal size of the spatial averaging region should be on the order of several building heights.

Buildings exert a drag force on the flow. The resulting shear stress has a maximum near the top of the buildings (Cheng and Castro, 2002; MacDonald, 2000) and then decreases to zero below the height of the buildings. The shear stress near the building tops is associated with a sharp gradient in the mean wind speed and the low shear stress within the urban canopy is associated with a nearly constant wind speed (with height) near the ground. Based on these observations, a simple approach to determine the wind speed within the canopy is to assume a constant (with height) wind speed. By matching the shear stress of the inertial sublayer with the drag force of the buildings, we can relate this wind speed with the parameters of the inertial sublayer and building geometry. Bentham and Britter (2003) developed a relationship between the constant spatially averaged canopy velocity, U_c, the surface friction velocity of the inertial sublayer above the urban area, u_*, and the frontal area fraction of the buildings:

$$\frac{U_c}{u_*} = \left(\frac{2}{\lambda_f}\right)^{1/2} \tag{5.1}$$

The wind within the UCL is often modeled using concepts similar to those of forest canopies. The work on modeling vegetation canopies has been translated for applications to the UCL by MacDonald (2000). By allowing the wind speed to vary with height, these models predict an exponential variation of the wind speed with height (MacDonald, 2000):

$$U(z) = U_H e^{(z-H)/l} \tag{5.2}$$

where U_H is the velocity at the building height and l is a length scale proportional to the building height that determines how deep the rooftop wind penetrates into the urban canopy. MacDonald derives relationships between these parameters and the building frontal and plan area fractions.

Another approach is to use empirical relationships between street and roof wind speed and turbulence. Several field experiments have provided data for this approach (Allwine et al., 2002; Hanna et al., 2007; Rotach et al., 2005).

Vortex Flow and Street Canyons

Some of the earliest studies of dispersion in cities were performed in 1970 and 1971 in San Jose, California, and St Louis, Missouri (Johnson et al., 1973). The studies resulted in a semiempirical dispersion model based on the Gaussian plume model along with a "submodel" that accounts for the microscale features of the dispersion within the urban street. The plume spreads for the Gaussian plume model were determined from tracer release field measurements in a study conducted in St Louis between 1963 and 1965.

The microscale model of (Johnson et al., 1973) and most semiempirical urban dispersion models are based on the picture of the "street canyon," a street with uniform height buildings on either side, a prototypical building block of the urban environment. Fig. 5.2 shows a schematic of a street canyon model. The ideal street canyon has buildings all the same height and no gaps between the buildings. Depending on the aspect ratio, the ratio of the height of buildings to the street width, and the rooftop wind speed and direction, a recirculating vortex flow can develop within the street (Oke, 1988). The physical picture of the dispersion within street canyons typically includes a model of the vortex flow. This model primarily determines the relationship between the near-road concentration and the governing meteorological variables.

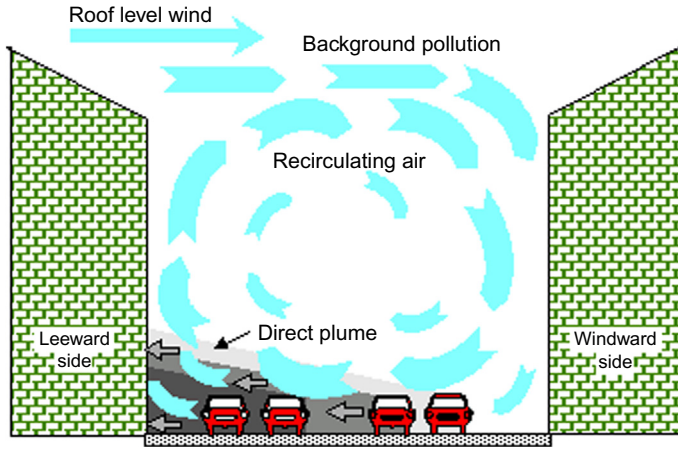

Figure 5.2 Berkowicz, R., 2000. OSPM — a parameterised street pollution model. Environ. Monit. Assess. 65, 323–331 (Figure 1. Schematic illustration of flow and dispersion conditions in street canyons.)

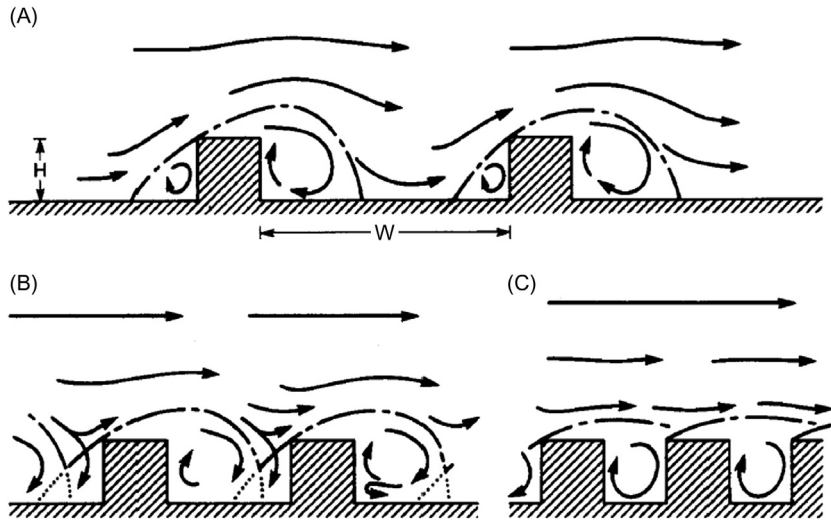

Figure 5.3 Building array flow regimes. (A) Isolated roughness flow; (B) wake interference flow; and (C) skimming flow. Taken from (Oke, 1988).

The existence of a vortex within the street canyon depends on the aspect ratio, the ratio of building height to street width. When the aspect ratio is small, no consistent vortex forms within the canyon, and when the aspect ratio is large, multiple vortices may form. Oke (1988) groups the flow regime within building arrays into the following classes based on

the canyon aspect ratio (Fig. 5.3): isolated roughness flow—the wakes downwind of individual obstacles do not interfere with each other; wake interference flow—the wakes behind obstacles are the same size as the distance between obstacles and begin to interfere with each other; skimming flow—a stable circulation forms within the canyon and the bulk of the flow does not enter the canyon.

For a long street canyon, the change from isolated roughness to wake interference flow occurs around an aspect ratio of 0.3, and the change from wake interference to skimming flow occurs around an aspect ratio of 0.75. The street canyon vortex may disappear under low ambient wind speeds. DePaul and Sheih (1986) verified the existence of a vortex flow using neutrally buoyant balloons as tracers. They found that the vortex disappears when the ambient wind speed is less than 1.5–2 m/s.

One early field study was conducted in a street canyon in San Jose, CA in 1973 (Johnson et al., 1973). Carbon monoxide concentrations and wind speed were measured at several locations and at five different heights within the canyon. The researchers found that the concentrations at the leeward side of the canyon were 3–4 ppm (33%–66%) larger than those at the windward side when the wind blows perpendicular to the canyon, while under parallel flow, the concentrations are similar at both sides. The vertical concentration gradient is smaller at the windward side. The authors show that the ground-level concentration at the leeward side is related to the rooftop wind speed, traffic count, and street geometry as follows:

$$C_L = C_b + \frac{0.07N}{(U + 0.5)(2 + x)} \tag{5.3}$$

where C_b is the background concentration, N is the traffic count, x is the distance from the traffic lane to the receptor, and U is the wind speed. A similar form holds for the windward side, with $2 + x$ replaced by the street width. The factor of 0.5 in the denominator accounts for the effect of vehicle induced turbulence. This model indicates that changes in building height do not directly alter the concentration, and only the street width and rooftop wind speed determine dispersion.

Wind tunnel models of street canyons have shown the same relationship between wind speed and pollutant dilution as was found in the previously mentioned field studies. Meroney et al. (1996) found that the concentration was inversely related to the approach wind speed. Barlow and Belcher (2002) found that the entrainment velocity that mixes pollutants vertically is proportional to the wind speed above the canyon. Both

studies tested the effect of increasing the surface roughness upstream of the canyon to simulate real urban conditions. Meroney et al. (1996) found that the presence of upstream buildings creates a displacement of the incoming velocity profile, which causes the formation of a shear layer at the top of the canyon and results in a permanent recirculating eddy within the canyon (with aspect ratio 1), while the small upstream roughness case shows an intermittent eddy for the same canyon. The presence of upstream buildings thus results in trapping of pollutants within the permanent recirculating eddy, resulting in larger concentrations relative to those in the absence of buildings. For smaller aspect ratios, the presence of upstream buildings is less important.

These studies show the importance of the rooftop wind speed in determining dispersion in street canyons. Other studies indicate that the vertical pollutant transport occurs due to an unstable shear layer that develops at the top of the canyon (Louka et al., 2000). The unsteady fluctuations of the shear layer cause intermittent recirculation in the canyon, thus intermittently flushing pollutants out of the canyon. The street canyon studied by Louka et al. (2000) was mostly isolated, with only three buildings upwind of the canyon. The reason for the very intermittent vortex flow in this experiment may be similar to that for the Meroney et al. (1996) wind tunnel study, where the isolated street canyon had a more unsteady vortex than the canyon surrounded by urban roughness.

Some of the existing work on modeling street canyons is summarized by Vardoulakis et al. (2003). Existing models can be classified as: empirical regression models, semiempirical box models, semiempirical Gaussian plume models, Lagrangian particle models, unsteady Gaussian puff models, and computational fluid dynamics (CFD) models. We are most interested in the semiempirical box and Gaussian plume models because they require only easily measured input variables and capture only the essential mechanisms of dispersion in cities. CFD models are capable of simulating dispersion in cities, but they do not provide clear insight into the important mechanisms.

Challenges for Practical Application of Models of Building Effects on Dispersion

There are several difficulties in applying semiempirical street canyon dispersion models to model dispersion in real-world cities. One problem with dispersion models based on the street canyon model is that it is not clear that they are applicable to real-world urban streets with significant

building height variability and spatial inhomogeneity. Well-known street canyon dispersion models have been evaluated mostly with data collected in European cities, where medium density urban streets tend to closely approximate the ideal street canyon. Dense urban cores within the United States have significant spatial and building height variability, putting into question the applicability of the street canyon dispersion models to these urban environments.

A further challenge facing application of urban dispersion models is that there is little consensus on the meteorological variables that are most relevant for application to near-road dispersion model parameterizations. The STREET model of Johnson et al. (1973), which is similar to the model of Dabberdt et al. (1973), parameterizes the concentration in terms of the near surface wind speed within the street, which is linearly related to the rooftop wind speed in the model formulation. Nicholson (1975) developed a model that parameterizes concentrations in terms of the average vertical velocity near the top of the street canyon when the wind is perpendicular to the street. For parallel winds, the average horizontal wind speed within the canyon is used. For conditions of low within-canyon wind speeds, the canyon plume box model (CPBM) of Yamartino and Wiegand (1986) parameterizes pollutant transport using a Gaussian plume model with plume spreads determined by the average vertical and horizontal turbulent velocities within the street canyon. The OSPM (Berkowicz et al., 1997) relates the surface concentration with both the vertical turbulent velocity near the surface and the roof of the canyon.

Vortex flow within a street canyon may result in higher concentrations on one side of the street than the other. Most street canyon models describe the spatial variation of concentrations within the street by accounting for the vortex flow that advects emissions from the street toward the leeward side (Berkowicz et al., 1997; Johnson et al., 1973; Yamartino and Wiegand, 1986). These models typically include a parameterization of the "recirculating" contribution, which affects the concentration on both the windward and leeward sides of the street, and is due to the vortex flow trapping pollutants within the canyon, and the "direct" contribution, which impacts on the leeward side of the street, due to direct emissions advected across the street. Other models such as that of Nicholson (1975) only parameterize the average concentration within the canyon. As mentioned previously, the vortex flow model may not be appropriate for cities with significant spatial inhomogeneity. We examine

the value of this aspect of the vortex flow concept as part of the dispersion model evaluation.

A significant challenge to the application of dispersion models to urban environments is the lack of routine measurements of the required meteorological data inputs. Because of this, models rely on assumptions about the relationships between available data and the required model inputs. The street canyon model of Dabberdt et al. (1973) parameterizes the concentration in terms of the rooftop wind speed. The rooftop wind speed used in the model is estimated from the wind speed measured at a nearby airport. This simple parameterization results from the need to use routinely measured wind speed as model inputs. Normally, only measurements of mean wind speed and direction are made at rural locations such as airports. Turbulence levels are not routinely measured, and even mean wind speed and direction data is usually not available within dense urban centers. For these reasons, all of the urban dispersion models require such parameterizations to be applicable to real world situations. The semiempirical models that we describe in this chapter are developed with the requirement that they only depend on meteorological data that are readily available or can be determined through semiempirical models that relate the wind speed measured at the "rural" airport site to that at the urban site of interest.

Primary Variables Governing Dispersion in Cities

We now examine the primary variables that govern near-road pollutant concentrations in cities. We present the discussion in the context of an analysis of near-road concentration data using several dispersion models. The relationship between vehicle-related concentrations in a street and associated micrometeorology was formulated through an analysis of data collected by the Lower Saxony Ministry for Environment, Energy, and Climate, in Göttinger Straße, Hanover, Germany, during 2003–2007. Göttinger Str. is 25 m wide with 20 m-tall buildings on either side. Measurements of NO and NO_2 concentrations were made at two locations: one on the southwest side of the road 1.5 m above ground level (AGL) and the other on the southwest building rooftop above the surface monitor. Wind speed and turbulence measurements were made using a sonic anemometer near the surface concentration monitor at 10 m AGL, and mean winds were measured near the rooftop monitor at 42 m AGL. Traffic flow measurements were made with automatic

counters, and were converted into emission rates using emission factors of 0.465 and 6.18 g/km of NO_x for passenger cars and trucks, respectively, determined using EMFAC 2007 (California Air Resources Board, 2017). We used the average emission factors for light and heavy duty trucks for the truck portion of the traffic and that for light-duty vehicles for the passenger car portion.

We used the Göttinger Strasse data to evaluate several alternative dispersion models with different dependence on the surface and rooftop σ_w and wind speed. We treat the rooftop concentration as the urban background, so that the difference between street and roof concentrations is the local contribution estimated by the models. We used the NO_x concentration measurements for model comparison because NO_x emission factors are relatively well known.

Our discussion of the variables governing dispersion in cities is framed in terms of an analysis of several alternative models. The first model is a modified form of the OSPM direct contribution model and is described by Eq. (5.4), where h_0 is the initial vertical plume spread, q is the emission rate per unit length of road, σ_{ws} is the near surface standard deviation of vertical velocity fluctuations, U_s is the near surface wind speed, W is the road width, and w is the distance of the receptor from the side of the road.

$$C = \sqrt{\frac{2}{\pi}} \frac{q}{W\sigma_{ws}} ln\left(1 + \frac{\sigma_{ws} W}{h_0 U_s + \sigma_{ws} w}\right) \tag{5.4}$$

If the initial vertical plume spread is negligible compared with the plume spread due to atmospheric turbulence at the position of the receptor, $\sigma_{ws} w / U_s h_0 >> 1$, then the direct concentration is described by Eq. (5.5), where a term with logarithmic dependence on the street width has been neglected.

$$C = \sqrt{\frac{2}{\pi}} \frac{q}{W\sigma_{ws}} \tag{5.5}$$

The models of Eqs. (5.4) and (5.5) are insensitive to the initial vertical plume spread. To examine the influence of the initial vertical plume spread, we assumed that the concentration is well mixed below the height h_0, and follows a Gaussian shape above h_0. Then the concentration near the surface is described by Eq. (5.6), where L is the length of the street upwind of the receptor.

$$C = \sqrt{\frac{2}{\pi}} \frac{q}{\sigma_{ws} w} \left(1 + \sqrt{\frac{2}{\pi}} \frac{h_0 U_s}{L \sigma_{ws}} \right)^{-1} \tag{5.6}$$

A comparison of model estimates from these three models with measurements from Gottinger Strasse showed that the simplest model, Eq. (5.5), provided the best description of the data. This equation is consistent with the scaling suggested by Kastner-Klein et al. (2003), who found that σ_w is a better scaling velocity than U_s for the concentration.

MODELS FOR THE EFFECTS OF BUILDINGS

The previous section described the important physical effects that buildings have on the transport of pollutants within cities. We now show how models of the dispersion of traffic emissions can be constructed. The discussion is focused on two models, the OSPM and the VDM. OSPM is widely used and is recognized as the state-of-the-art operational near-road dispersion model by the European air pollution research community within which it was developed. It has been evaluated extensively with observed concentrations of traffic emissions in several cities, primarily in Europe. The model design is based on the idealized street canyon formulation, commonly found in the cities of Europe from which the model originated. However, this may limit the models usefulness for streets that do not fit the assumptions of the street canyon model. The second model, VDM, is designed to estimate dispersion in streets characterized by non-uniform building heights and spatial inhomogeneity, features characteristic of cities in North America.

Operational Street Pollution Model

OSPM combines a street canyon box model with a model of the dispersion of the direct emissions from the road. The recirculating vortex flow advects emissions from the road toward the leeward side of the street. The emissions are then mixed vertically, and are trapped within the canyon by the vortex flow. Exchange of the trapped pollutants with the air above the canyon occurs by vertical turbulent transport, the magnitude of which is controlled by the standard deviation of vertical velocity

fluctuations at the roof level. To model these features of the dispersion, OSPM separates the concentration into two components: the recirculating component and the direct component (see Fig. 5.2).

For the direct component, the vertical plume spread, σ_z, is given by:

$$\sigma_z = h_0 + \sigma_{ws} x / U_s \tag{5.7}$$

where σ_{ws} is the vertical turbulent velocity at the bottom of the canyon, U_s is the wind speed at the bottom of the canyon, and h_0 is the initial vertical plume spread. By modeling the road as an area source and integrating the ground-level concentration across the source, the concentration next to the edge of the road is given by Berkowicz et al. (1997):

$$C_{direct} = \sqrt{\frac{2}{\pi}} \frac{q}{W \sigma_{ws}} \ln\left(1 + \frac{W \sigma_{ws}}{h_0 U_s}\right) \tag{5.8}$$

where q is the emission rate per unit length of road and W is the road width. The initial vertical plume spread, h_0, is due to the mixing produced by motion of the vehicles, and has magnitude proportional to the vehicle height.

The recirculating contribution is determined by considering the canyon as a box model. Emissions enter the box at the bottom and are transported out of the box at the top by the vertical turbulent velocity at the top of the box. When the building height, H, is larger than the street width, $H \geq W$, the concentration in the box is:

$$C_{recirc} = \frac{q}{W \sigma_{wr}} \tag{5.9}$$

where σ_{wr} is the standard deviation of vertical velocity fluctuations at the top of the canyon.

OSPM determines the wind speed at the bottom of the canyon from that at the rooftop by assuming a logarithmic velocity profile within the canyon:

$$U_s = U_t \frac{\ln(h_0 / z_0)}{\ln(H / z_0)} (1 - 0.2 p \sin(\Phi)) \tag{5.10}$$

where U_t is the wind speed at the top of the canyon, z_0 is the surface roughness length, Φ is the angle of the rooftop wind from the direction parallel to the street, and $p = H_{upwind}/H$, where H_{upwind} is the building height on the upwind side of the road. The surface roughness length is

0.1 m. At the ground, the vertical turbulent velocity is the combination of the mechanically generated turbulence and the traffic produced turbulence:

$$\sigma_{ws} = ((0.1U_s)^2 + \sigma_{w0}^2)^{1/2} \tag{5.11}$$

where σ_{w0} is the vertical turbulent velocity due to traffic. The vertical turbulent velocity at the roof is calculated as:

$$\sigma_{wr} = ((0.1U_t)^2 + 0.4\sigma_{w0}^2)^{1/2} \tag{5.12}$$

The traffic produced turbulence is:

$$\sigma_{w0} = b\left(\frac{N_{veh}VS^2}{W}\right)^{1/2} \tag{5.13}$$

where N_{veh} is the traffic flow rate, V is the average vehicle speed, S^2 is the surface area of one vehicle, and $b = 0.3$ is a constant.

OSPM includes many special cases and formulations to ensure that the concentrations produced by the model are reasonable. The description of OSPM that we have given here only includes the components of the model essential to describe the street canyon formulation for winds blowing perpendicular to the street.

Vertical Dispersion Model

OSPM is designed to estimate concentrations within street canyons and thus invokes the concept of a street lined with unbroken walls of buildings with uniform heights. Within real-world cities, the building heights and shapes are often extremely variable, buildings are placed at varying distance from the road, and gaps often exist between buildings. It is not clear that street canyon models are useful for estimating dispersion of traffic emissions within these types of streets, which are typical of those found in US cities. Thus, there is a need for a model that accounts for the effects of varying building heights on dispersion. But, in doing so, as we will see later, the model relinquishes the spatial resolution of the concentration field that OSPM is designed for.

The model that we describe next is designed to estimate near surface concentrations of pollutants emitted from vehicles traveling on urban streets

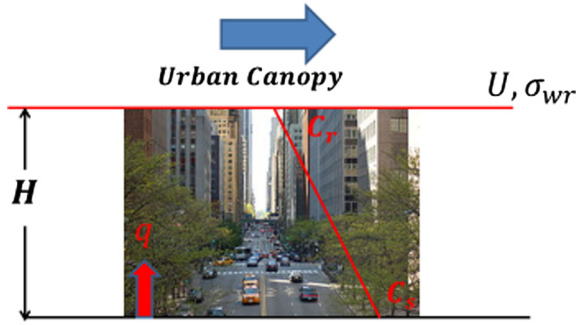

Figure 5.4 Schematic illustrating the balance between emissions and vertical transport.

surrounded by buildings. We refer to it as the vertical dispersion model (VDM) to emphasize the dominant influence of vertical turbulent transport in its formulation. The model assumes that the near surface concentrations over the length and breadth of a typical city block is governed by the balance between emissions at the surface and vertical transport out of the urban canopy, as shown in Fig. 5.4.

Then, we can write

$$q \sim K_z W \frac{(C_s - C_r)}{H} \tag{5.14}$$

where K_z is the vertical eddy diffusivity, H and W are the building height and street width, C_s is the horizontally averaged concentration in the street canyon at the ground, C_r is the rooftop (at H) concentration, and q is the emission rate per unit length of the street.

The eddy diffusivity is taken as the product of a mixing length, l, and the standard deviation of vertical velocity fluctuations averaged over the height of the buildings, σ_w:

$$K_z = l\sigma_w \tag{5.15}$$

If we assume that the size of the large turbulent eddies dominating vertical mixing is limited by the smaller of the street width and building height, then the mixing length is proportional to the smaller of H and W:

$$l \sim \left(h_0 + \frac{HW}{H + W} \right) \tag{5.16}$$

where h_0 is the mixing length associated with the initial vertical mixing caused by the motion of the vehicles. Eqs. (5.14) through (5.16) can be combined to yield an expression for the surface concentration:

$$C_s - C_r = \frac{q}{\beta\sigma_w W}\left(\frac{1+a_r}{1+(1+a_r)\left(h_0/H\right)}\right) \tag{5.17}$$

where $a_r = \left(H/W\right)$ is the aspect ratio and β is an empirical constant, which is obtained by fitting model estimates to observations.

If measurements of the rooftop concentration are not available, C_r can be estimated by assuming that local emissions are matched by vertical transport at roof level:

$$q = \gamma C_r W \sigma_{wr} \tag{5.18}$$

where $\sigma_{wr}$is the standard deviation of vertical velocity fluctuations at roof level, and γ is an empirical constant used to calibrate the model.

Substituting Eq. (5.18) into (5.17) yields:

$$C_s = \frac{q}{\gamma\sigma_{wr} w}\left(1 + \frac{\gamma\sigma_{wr}}{\beta\sigma_w}\frac{1+a_r}{1+(1+a_r)\left(\frac{h_0}{H}\right)}\right) \tag{5.19}$$

Eqs. (5.17) and (5.19) are referred to as the VDM. Eq. (5.17) can be used if σ_w and C_r can be estimated from measurements. In practice, this information is usually not available. Thus, it is often necessary to estimate the average σ_w from the rooftop σ_{wr}, which can be estimated using the models described in Chapter 6.

We can relate σ_w to σ_{wr} by assuming that turbulent kinetic energy produced at roof level, per unit length of street, $u_{*r}^2 U_r W$, is dissipated over the volume of the street at the rate $(\sigma_w^3/l)WH$:

$$u_{*r}^2 U_r W \sim \sigma_{wr}^3 W \sim \frac{\sigma_w^3}{l} WH \tag{5.20}$$

where l is the length scale of the large turbulent eddies within the canyon, and u_{*r}^2 and U_r are the shear stress and the mean wind speed at roof level, and both u_{*r} and U_r are correlated with σ_{wr}. If l is similar to the form given by Eq. (5.16), we can write the semiempirical expression:

$$\sigma_{wr} = \sigma_w(1+\eta a_r)^{1/3} \tag{5.21}$$

where $\eta = 0.4$ provides the best fit with the data as shown in a later section. The ratio of rooftop and average σ_w is nearly constant because the 1/3 power in Eq. (5.21) results in low sensitivity to the aspect ratio.

The application of VDM requires a value of the aspect ratio, a_r, that best describes the morphology of the nonuniform buildings lining a street. This was determined empirically by evaluating VDM with data collected in a field experiment conducted in Los Angeles, the details of which are discussed in the next section. We found that the following definition of the effective height, H, of the buildings provided the best results:

$$H = \frac{1}{L}\sum_i H_i B_i \tag{5.22}$$

where L is the street length, H_i and B_i are the height and width (along the street) of building i, and the sum is taken over all the buildings on one side of the street. Eq. (5.22) can be interpreted as the area-weighted building height: the sum of the frontal area of the buildings divided by the street length. Then, the equivalent building height used in Eq. (5.19) is the average over both sides of the street.

We assume that the modeled concentration represents an average over the street canyon within one city block. For the effective building height to be consistent with the model, it is calculated from the geometry of all the buildings bordering the street canyon within one city block. The use of the block length for defining the scale for horizontal inhomogeneity is somewhat arbitrary, but the assumption of horizontal homogeneity within one city block has been used in models such as SIRANE (Soulhac et al., 2011), and comparisons with observations indicate that this is a useful assumption.

COMPARISON OF MODEL WITH OBSERVATIONS

This section describes the performance of the VDM in estimating concentrations of traffic emissions. Model performance is evaluated using near-road measurements of concentrations of ultrafine particle number (UFP) and carbon monoxide (CO) made in field studies conducted in Riverside and Los Angeles, CA.

Throughout this section, we use the geometric mean, m_g, and standard deviation, s_g, of the residuals between log-transformed model predictions and observations as well as the correlation coefficient, r^2, and the fraction of data within a factor of two of model estimates, *fact*2, to evaluate model performance. The geometric mean and standard deviation are computed as $\ln(m_g) = \frac{1}{n}\sum_i r_i$, and $\ln(s_g) = \sqrt{\frac{\sum_i [r_i - \ln(m_g)]^2}{n-1}}$, where $r_i = \ln(C_{oi}) - \ln(C_{mi})$, subscripts *oi* and *mi* refer to observed and model estimated concentrations, and n is the number of data points. An m_g equal to one indicates zero model bias. The interval that contains 95% of the ratios of observed to predicted concentrations is approximately given by $[m_g s_g^{-2}, m_g s_g^2]$.

Description of the Los Angeles Field Measurements

We use observed near-road concentrations of UFP to evaluate the dispersion models. This is done for three reasons. First, UFP is a product of combustion that provides a strong signal of local traffic emissions. Second, it is linked with negative health effects (Knibbs et al., 2011). Finally, the condensation particle counters that measure UFP have a response time on the order of 10 s, fast enough to capture the impact of individual vehicles or groups of vehicles on the concentration. The time signature of these concentration events can be processed to yield the contribution of local vehicle traffic on the total concentration observed by the monitor. Thus, the UFP signal allows us to separate local traffic sources from background sources, which is extremely useful for evaluation of street-scale dispersion models since these models use horizontal averaging scales on the order of the size of the street and thus treat emissions on adjacent streets as part of the background.

The primary condition for locating the concentration monitors is based on the need to resolve the effect of the built environment on near road concentrations. Field measurements pose significant challenges to isolating the effect of one variable on the concentration because variability in uncontrolled factors such as traffic emission rate can overwhelm the signal due to the presence of buildings. The local vehicle emission rate must be known to evaluate the dispersion models, but emissions can be difficult to determine in practice. Individual vehicle emission rates can vary significantly, and during congested driving conditions, characteristic of urban environments, the local traffic within a street is often

Table 5.1 Locations at Which Field Measurements of UFP Were Made. The Observations Are Used to Evaluate the VDM and OSPM

Location	Dates	Building Morphology
Downtown Los Angeles	9/20/13, 5/7/14, 5/9/14	Urban core with significant building height variability. Many buildings approximately 50 m tall
Wilshire Blvd	5/30/14	Variable building heights up to 50 m tall. Average building height is less than that in downtown Los Angeles
Temple City	1/15/14, 1/16/14, 1/17/14	Suburban area with many single-story buildings. Nearly uniform building height of 6 m
Riverside	7/1/15–7/30/15	Urban area with buildings about 20 m tall

accelerating or idling, increasing uncertainty of the emission rates (Smit et al., 2008). Emission models of gaseous pollutants and particle mass are usually accurate to about a factor of two or three (Smit et al., 2010). UFP number, which we use as the primary measured pollutant in the field study, has emission factors that vary by about an order of magnitude Kumar et al. (2011). Because of the uncertainty in the emission estimates, when possible the experiments were designed so that UFP concentration measurements were made at two sections on the same street: one section with tall buildings adjacent to the street and another where there are no buildings or very short buildings adjacent. This design ensures that local vehicle emissions are similar at the two locations, allowing us to directly compare concentrations at the open and building sections to isolate the building effect.

The data used in this evaluation was collected during two measurement campaigns. The first campaign was conducted in several cities in Los Angeles County, CA, USA, between September 2013 and July 2014. The second campaign was conducted in Riverside, CA, USA, in September and August, 2015. Table 5.1 gives an overview of the building morphology of the various field locations in this campaign.

Here, we use the data from the Los Angeles study to evaluate the performance of the VDM and OSPM. We use data from the Riverside field study to further evaluate the VDM, including observed concentrations of traffic-emitted carbon monoxide. The evaluation using the data from the Riverside study is described in the next section.

Table 5.2 Summary of Area-Weighted Building Height, Street Width, and Aspect Ratio of All Sites

Site	Area-Weighted Building Height [m]	Street Width [m]	Aspect Ratio
8th St Building	43.25	20.0	2.16
8th St Mid	34.5	20.0	1.73
Broadway	35.90	26.0	1.38
7th St	45.80	25.0	1.83
Temple City	6.00	30.0	0.20
Wilshire Blvd Building	36.0	30.0	1.20
Wilshire Blvd Open	8.25	30.0	0.28

TSI 3022 condensation particle counters were used to record UFP number concentrations at a sampling rate of 1 Hz. Samples are drawn through a copper and Tygon tube with the tube sampling inlet set at 1 m above ground level. The instruments measure the concentration of particles with diameters greater than 10 nm (50% detection efficiency is 10 nm). The inlet flow rate is 1.5 L min^{-1}.

One of the measurement locations in downtown Los Angeles was near the 8th St and Hill St intersection. The site was chosen because 8th St had a section where there were no buildings next to the road, the "open" site, and a section where there were tall buildings directly next to the road, the "built" site. We obtained building height and outline information for Los Angeles County in a GIS database format which we then used to calculate the built environment parameters shown in Table 5.2. The data for this study was obtained from the Los Angeles County GIS data portal (Los Angeles County, 2008). Information about the building geometry is an essential component for modeling dispersion of traffic emissions that is often not readily available. It is rare to have access to such information on the built environment as LA county freely provides.

Evaluation of the VDM with Data Collected in Los Angeles and Riverside

Fig. 5.5 shows the evaluation of the surface concentration predicted by Eq. (5.19) with the 30-min averaged local contribution of UFP in the Los Angeles field study, normalized by the traffic emission rate based on the local vehicle traffic counts. The local contribution is a measure of local traffic impacts, and we use the average of the values measured on

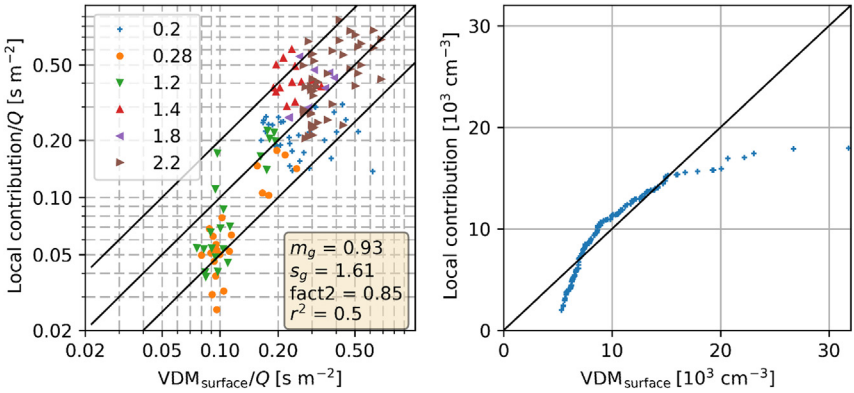

Figure 5.5 Comparison of VDM with 30 min averaged local contribution of UFP. Left: scatter plot of the data. The local contribution is the average of both sides of the street and is normalized by the daily average emission rate, assuming an emission factor of $10^{14} veh^{-1} km^{-1}$. Right: quantile−quantile plot. The building height of the 8th St open section has been set equal to that of the 8th St building section. $\text{VDM}_{surface}$ is C_s from Eq. (5.19).

both sides of the street for the model evaluation. We describe the method to compute the local contribution next.

To remove the impact of background sources, we determine the contribution of local emissions to the total concentration observed at the surface monitors, and use only this "local contribution." The UFP concentration time series contains information about the local vehicle emissions in the form of large amplitude short-lived spikes superimposed on the slowly varying baseline. This occurs because the UFP emission factor varies by several orders of magnitude, and so local emission events from high-emitting vehicles produce large concentration spikes that can be separated from the total concentration. We filter the signal to separate the slowly varying component from the spikes, which contain information about local emissions. A moving average filter with a window size larger than the time scale of the spikes does not adequately separate the two components because the concentration distribution is highly skewed, making the average an inadequate measure of the baseline concentration. Instead of the moving average, we use a windowed percentile to separate the components. We define the baseline as the concentration that is below a chosen percentile of the concentration distribution. Then, within each time window of a chosen length, each data point is classified as either baseline or spike if the concentration is below or above the

percentile cutoff of the window. The baseline is then constructed by linearly interpolating between the points that are classified as baseline, and the spikes are separated by subtracting the baseline from the total. This type of analysis is common for analyzing UFP time series, especially in analysis of mobile monitoring data (Bukowiecki et al., 2002). Details of the method that we have developed are described in Schulte et al. (2015).

The model was applied to the data using the best fit parameters $h_0 = 2m$ and $\beta = 1$. The values of the parameters that characterize the buildings, the area-weighted building height, and street width are listed in Table 5.2. We have assumed the emission factor of UFP equals $10^{14} veh^{-1} km^{-1}$, which is the magnitude of UFP emission factors reported in literature (Kumar et al., 2011). The value of the final parameter, γ, was determined by matching the observed and modeled concentrations from the Los Angeles data. The resulting value is $\gamma = 1.0$.

The left panel of Fig. 5.5 shows the scatter plot of the data and the right panel shows a quantile−quantile plot. The figure indicates that the model provides a good description of the measured local contributions of UFP. There is little model bias and most of the observations are within a factor of two of the model estimates. The quantile−quantile plot indicates that the model overestimates the lowest concentrations and the scatter plot of the concentrations normalized by emissions shows that this is due to underestimation of the dispersion. However, most of the data is described well by the model. This implies that local contributions are primarily governed by the ratio of area-weighted building height to street width and the vertical average of the standard deviation of the vertical velocity fluctuations. The low model bias indicates that traffic emissions are consistent with an emission factor of $1.0 \times 10^{14} veh^{-1} km^{-1}$. This value is within the range reported by Ketzel et al. (2003).

Evaluation of the OSPM recirculating contribution model, which uses the mean rooftop wind speed as the primary meteorological variable governing near road concentrations, showed little correlation between model estimates and observations at the field sites in the Los Angeles study. This supports the conclusion that vertical turbulent transport rather than advection by the mean wind dominates dispersion in cities with significant building height variability. This conclusion is supported by observations analyzed in Hanna et al. (2014), which show that data from field studies conducted in Manhattan, NY, indicate rapid vertical mixing in the presence of buildings.

We show that modeling the air quality impact of vehicular emissions reduces to estimating the effective aspect ratio of the street, and the roof

level σ_w. The effective aspect ratio plays the major role in magnifying concentrations relative to those that would have been measured in the absence of buildings.

The building morphology where measurements were conducted in Los Angeles was mainly of two types: urban core areas with many tall (~50 m) buildings, and suburban with primarily single story buildings. So VDM was evaluated with measurements conducted in a street with an intermediate aspect ratio of 0.4 in Riverside, CA, over a period of about a month. We used observed near-road concentrations of carbon monoxide to improve the calibration of the empirical constants in the VDM and to estimate confidence limits for their values.

As in the previous study conducted in Los Angeles, concentration measurements were made next to a busy road at two locations, one with tall buildings next to the road and one several blocks away with only short buildings next to the road. A site next to Market St in Riverside, CA, was chosen to meet the requirements of the study. Fig. 5.6 shows an overview of the site. The "building" section has an area-weighted building height of 14.37 m and a street width of 33 m, resulting in an aspect ratio of 0.44. The "open" section has area-weighted building height of 2.14 m and street width of 30 m. The traffic on Market St was about 26,000 vehicles per day.

Fig. 5.6 shows the locations of the instruments that were used in the study. Campbell scientific CSAT3 sonic anemometers were used to measure the three components of wind speed and temperature at 10 Hz at both the building and open sites and on the roof of city hall, approximately 100 m from the building site. The resulting turbulence data was processed to yield time average wind speeds, wind direction, turbulent velocities, and heat and momentum fluxes. The micrometeorological measurements were made continuously between July 30 and September 9, 2015.

Concentrations of UFP were measured using TSI 3022 condensation particle counters between about 7 am and 7 pm on 15 days in August and September, 2015, resulting in a total of about 150 h of particle concentration data. A total of five particle counters were used: one on each side of Market St at both the building and open sites and one on the city hall roof. The instruments provided 1-second average concentrations. The UFP concentration data was processed to yield the contribution of local vehicle traffic using the method described for the evaluation of the Los Angeles data.

Figure 5.6 Location of instruments in May 2015 Riverside, CA, field study. ●—Condensation Particle Counter (CPC).●—AQMesh. △—Sonic Anemometer. ■—Camera. Map Data: Google.

Measurements of carbon monoxide (CO), nitrogen oxides (NO and NO_2), ozone (O_3), and sulfur dioxide (SO_2) were made using AQMesh five gas pollutant monitor "pods" between August 18 and September 9, 2015. The pods are ideally suited for long term measurements of concentrations of vehicle emissions. They use much less power than the condensation particle counters, the integrated battery holds enough charge to function for the entire study, enabling continuous concentration measurements. Three pods were used: one on each side of Market St at the "building" section, and one on the rooftop. Averaging time for the AQMesh monitors was 1 min, and data was later aggregated into 2 h averages for analysis. Only the carbon monoxide data was analyzed for the evaluations in this chapter.

Sonic anemometers and AQMesh pods were mounted at a height of 4 m above ground level (AGL). Condensation particle counters mounted to light poles have inlets at a height of 1 m AGL. The rooftop sonic anemometer and AQMesh pod were attached to a tripod 3 and 2 m above the 25 m-tall roof of city hall, respectively. The rooftop condensation particle counter inlet is 0.5 m above the rooftop.

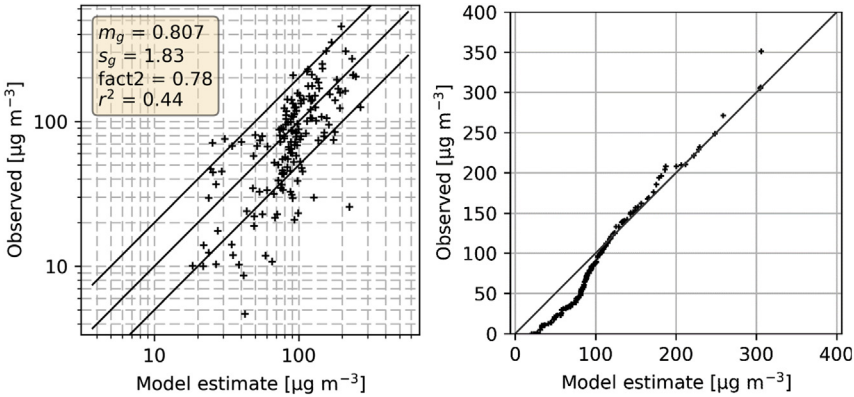

Figure 5.7 Comparison of VDM with vertical difference of 2-h average carbon monoxide concentrations in Riverside, CA. Left: Scatter plot of the data. Observations are normalized by the emission rate assuming an emission factor of 3.75$g\ km^{-1}$ for nontrucks and 2.5$g\ km^{-1}$ for trucks. Right: Quantile–quantile plot.

Fig. 5.7 shows the comparison of the observed vertical difference of carbon monoxide concentrations with VDM predictions. Model estimates are determined using emission factors of 3.75$g\ km^{-1}$ for nontrucks and 2.5$g\ km^{-1}$ for trucks.

There is significant scatter between the observations and model estimates, indicated by the low correlation coefficient. However, 78% of the data are within a factor of two of model estimates. Most of the discrepancy between observations and model estimates is due to cases where the observed vertical difference is small compared with model estimates. This usually occurs during night and early morning between about 1:00 am and 7:00 am, when the traffic flow rate and hence the emission rate is very small. We do not have a good estimate of the actual traffic flow rate during this time period. In particular, the comparison is somewhat sensitive to the assumption of when the morning rush hour traffic begins, since this determines the time of the morning spike in concentration. The right panel of Fig. 5.7 shows that the VDM tends to overestimate the lowest concentrations but otherwise the distribution of concentrations predicted by VDM describes the data remarkably well.

There is little model bias since we derived the emission factor from the comparison of model with observations. The values of m_g and s_g indicate that 95% of the observations are within a factor of 0.24–2.7 of the model estimates. These results show that the VDM adequately predicts near road

concentrations within an urban area. To apply the model, we need to determine the value of the meteorological input variables: σ_w at the urban rooftop and surface. Since measurements of σ_w are not routinely made in urban areas, these variables must be determined from routine meteorological measurements, which are usually only made in rural areas such as airports. Chapter 6 describes the evaluation of a model that relates measured micrometeorology at a rural area to that at the urban rooftop and surface.

SUMMARY

The evaluation of the VDM supports the applicability of the model for estimating near-road concentrations within urban areas. The results show that the standard deviation of vertical velocity fluctuations, σ_w, in the urban canopy governs near-surface concentrations, especially during low wind speed conditions typical of urban areas. The mean wind speed likely plays a small role in dispersion in urban areas because the turbulent intensities are large, resulting in significant horizontal meandering of the pollutant plume. Measurements of mean winds and turbulence in Manhattan and Oklahoma city (Hanna, 2009; Hanna et al., 2007) support the conclusion that strong vertical turbulent mixing governs dispersion in urban areas. Near surface winds in these studies were only about 1/3 of the rooftop value, and wind directions varied significantly (Hanna et al., 2007). This results in more horizontal meandering of pollutant plumes, creating conditions where vertical transport governs the near-road concentrations.

For the VDM to be consistent with the data collected in the Los Angeles study as well as the Riverside measurements, it was necessary to assume that the emission factors of NO_x, CO, and UFP could vary by about a factor of two of the EMFAC2011 estimates. This assumption is supported by studies showing errors in emission models of up to a factor of three and two for CO and NO_x, respectively (Smit et al., 2010). Emission factors depend on the composition of the vehicle fleet and the type of driving conditions. Hence, traffic flow conditions observed in the Riverside study may result in emission factors that are different from those predicted by average speed models such as EMFAC, and it may be necessary to estimate emissions by explicitly

including the level of traffic congestion at the field site in the emission model (Smit et al., 2008). However, it may be difficult to obtain more accurate emission estimates even with more comprehensive models that include measures of congestion because it will be more difficult to obtain accurate estimates of the input data for these models. Considering the uncertainty in the emission rates, the value of the model calibration constant β is likely within about a factor of two of the value $\beta = 1$ chosen in this study.

We have shown that estimating the impact of buildings on dispersion of traffic emissions in the near-road environment reduces to estimating the ratio of the area-weighted building height to street width and the vertical average of the standard deviation of vertical velocity fluctuations. Throughout this chapter, we have used measurements to determine the values of the micrometeorological model inputs. However, only the mean wind is routinely measured, and these measurements are primarily made in rural areas. For practical applications where the turbulence data in the urban area is unknown, we must determine the values of the micrometeorological input variables required for the VDM from these routine measurements. Chapter 6 describes methods to estimate the urban micrometeorology based on the routine measurements at an upwind rural location.

The evaluation and application of VDM has focused on a single street in a city block. How do we apply the model to estimate near surface concentrations in an urban area with a large number of roads? One approach is to use a model such as AERMOD to estimate concentrations at the effective top of the urban canopy assuming that the roads are the same level as the canopy top. The meteorological inputs would account for the roughness of the urban area averaged over the scale of the urban built-up area. The IBL model, described in Chapter 6, can be used to estimate these inputs. The resulting concentrations correspond to the rooftop values in Eq. (5.17), which can be then used to estimate the concentration at street level using

$$C_s = C_{AERMOD} + \frac{q}{\beta \sigma_w W}\left(\frac{1 + a_r}{1 + (1 + a_r)\left(h_0/H\right)}\right), \tag{5.23}$$

where the parameters in the second term on the right-hand side of the equation correspond to the road of interest. More details are described in Chapter 6.

REFERENCES

Aarhus University Department of Environmental Science, 2018. Operational Street Pollution Model-OSPM. http://www.au.dk/ospm/.

Allwine, K.J., Shinn, J.H., Streit, G.E., Clawson, K.L., Brown, M., 2002. Overview of urban 2000: a multiscale field study of dispersion through an urban environment. Bull. Am. Meteorol. Soc. 83, 521–536.

Barlow, J.F., Belcher, S.E., 2002. A wind tunnel model for quantifying fluxes in the urban boundary layer. Bound.-Layer Meteorol 104, 131–150.

Bentham, T., Britter, R., 2003. Spatially averaged flow within obstacle arrays. Atmos. Environ. 37, 2037–2043. Available from: https://doi.org/10.1016/S1352-2310(03)00123-7.

Berkowicz, R., Hertel, O., Larsen, S.E., Sørensen, N.N., Nielsen, M., 1997. Modelling traffic pollution in streets. Natl. Environ. Res. Inst. Rosk. Den 10129, 20.

Britter, R.E., Hanna, S.R., 2003. Flow and dispersion in urban areas. Annu. Rev. Fluid Mech. 35, 469–496. Available from: https://doi.org/10.1146/annurev.fluid.35.101101.161147.

Bukowiecki, N., Dommen, J., Prevot, A.S.H., Richter, R., Weingartner, E., Baltensperger, U., 2002. A mobile pollutant measurement laboratory—measuring gas phase and aerosol ambient concentrations with high spatial and temporal resolution. Atmos. Environ. 36, 5569–5579.

California Air Resources Board, 2017. Mobile Source Emission Inventory. URL https://www.arb.ca.gov/msei/msei.htm (accessed 1.1.17).

Cheng, H., Castro, I.P., 2002. Near wall flow over urban-like roughness. Bound.-Layer Meteorol 104, 229–259.

Cimorelli, A.J., Perry, S.G., Venkatram, A., Weil, J.C., Paine, R.J., Wilson, R.B., Lee, R.F., Peters, W.D., Brode, R.W., 2005. AERMOD: a dispersion model for industrial source applications. Part I: general model formulation and boundary layer characterization. J. Appl. Meteorol 44 (5), 682–693.

Dabberdt, W.F., Ludwig, F.L., Johnson, Jr., W.B., 1973. Validation and applications of an urban diffusion model for vehicular pollutants. Atmos. Environ. 7, 603–618.

DePaul, F.T., Sheih, C.M., 1986. Measurements of wind velocities in a street canyon. Atmos. Environ. 20, 455–459. Available from: https://doi.org/10.1016/0004-6981(86)90085-5.

Fisher, B., Kukkonen, J., Piringer, M., Rotach, M.W., Schatzmann, M., 2006. Meteorology applied to urban air pollution problems: concepts from COST 715. Atmospheric. Chem. Phys. 6, 555–564. Available from: https://doi.org/10.5194/acp-6-555-2006.

Hanna, S., 2009. A simple urban dispersion model tested with tracer data from Oklahoma City and Manhattan. Atmos. Environ. 43, 778–786.

Hanna, S., White, J., Zhou, Y., 2007. Observed winds, turbulence, and dispersion in built-up downtown areas of Oklahoma City and Manhattan. Bound.-Layer Meteorol. 125, 441–468. Available from: https://doi.org/10.1007/s10546-007-9197-2.

Hanna, S., Chang, J.C., Flaherty, J., 2014. Observed Ratios of Rooftop to Surface Concentrations in Built-Up City Centers. Atlanta, Georgia. Available at www.ametsoc.org.

Johnson, W.B., Ludwig, F.L., Dabberdt, W.F., Allen, R.J., 1973. An urban diffusion simulation model for carbon monoxide. J. Air Pollut. Control Assoc. 23, 490–498. Available from: https://doi.org/10.1080/00022470.1973.10469794.

Ketzel, M., Wåhlin, P., Berkowicz, R., Palmgren, F., 2003. Particle and trace gas emission factors under urban driving conditions in Copenhagen based on street and roof-level observations. Atmos. Environ. 37, 2735–2749. Available from: https://doi.org/10.1016/S1352-2310(03)00245-0.

Knibbs, L.D., Cole-Hunter, T., Morawska, L., 2011. A review of commuter exposure to ultrafine particles and its health effects. Atmos. Environ. 45, 2611–2622. Available from: https://doi.org/10.1016/j.atmosenv.2011.02.065.

Kumar, P., Ketzel, M., Vardoulakis, S., Pirjola, L., Britter, R., 2011. Dynamics and dispersion modelling of nanoparticles from road traffic in the urban atmospheric environment—a review. J. Aerosol Sci. 42, 580–603. Available from: https://doi.org/10.1016/j.jaerosci.2011.06.001.

Los Angeles County, 2008. Countywide Building Outlines.

Louka, P., Belcher, S.E., Harrison, R.G., 2000. Coupling between air flow in streets and the well-developed boundary layer aloft. Atmos. Environ. 34, 2613–2621.

MacDonald, R.W., 2000. Modelling the mean velocity profile in the urban canopy layer. Bound.-Layer Meteorol. 97, 25–45.

Meroney, R.N., Pavageau, M., Rafailidis, S., Schatzmann, M., 1996. Study of line source characteristics for 2-D physical modelling of pollutant dispersion in street canyons. J. Wind Eng. Ind. Aerodyn. 62, 37–56.

Nicholson, S.E., 1975. A pollution model for street-level air. Atmos. Environ. 9, 19–31.

Oke, T.R., 1988. Street design and urban canopy layer climate. Energy Build. 11, 103–113. Available from: https://doi.org/10.1016/0378-7788(88)90026-6.

Rotach, M.W., Vogt, R., Bernhofer, C., Batchvarova, E., Christen, A., Clappier, A., et al., 2005. BUBBLE – an urban boundary layer meteorology project. Theor. Appl. Climatol. 81, 231–261. Available from: https://doi.org/10.1007/s00704-004-0117-9.

Smit, R., Brown, A.L., Chan, Y.C., 2008. Do air pollution emissions and fuel consumption models for roadways include the effects of congestion in the roadway traffic flow? Environ. Model. Softw. 23, 1262–1270. Available from: https://doi.org/10.1016/j.envsoft.2008.03.001.

Smit, R., Ntziachristos, L., Boulter, P., 2010. Validation of road vehicle and traffic emission models – a review and meta-analysis. Atmos. Environ. 44, 2943–2953. Available from: https://doi.org/10.1016/j.atmosenv.2010.05.022.

Soulhac, L., Salizzoni, P., Cierco, F.-X., Perkins, R., 2011. The model SIRANE for atmospheric urban pollutant dispersion; part I, presentation of the model. Atmos. Environ. 45, 7379–7395. Available from: https://doi.org/10.1016/j.atmosenv.2011.07.008.

Vardoulakis, S., Fisher, B.E., Pericleous, K., Gonzalez-Flesca, N., 2003. Modelling air quality in street canyons: a review. Atmos. Environ. 37, 155–182. Available from: https://doi.org/10.1016/S1352-2310(02)00857-9.

Yamartino, R.J., Wiegand, G., 1986. Development and evaluation of simple models for the flow, turbulence and pollutant concentration fields within an urban street canyon. Atmos. Environ. 20, 2137–2156. Available from: https://doi.org/10.1016/0004-6981(86)90307-0.

FURTHER READING

Berkowicz, R., 2000. A simple model for urban background pollution. Environ. Monit. Assess. 65, 259–267.

Caton, F., Britter, R.E., Dalziel, S., 2003. Dispersion mechanisms in a street canyon. Atmos. Environ. 37, 693–702. Available from: https://doi.org/10.1016/S1352-2310(02)00830-0.

DePaul, F.T., Sheih, C.M., 1985. A tracer study of dispersion in an urban street canyon. Atmos. Environ. 19, 555–559.

Hanna, S.R., 1989. Confidence limits for air quality model evaluations, as estimated by bootstrap and jackknife resampling methods. Atmospheric Environ 1967 (23), 1385–1398.

Hoydysh, W.G., Dabberdt, W.F., 1988. Kinematics and dispersion characteristics of flows in asymmetric street canyons. Atmos. Environ. 22, 2677–2689.

Macdonald, R.W., Griffiths, R.F., Hall, D.J., 1998. An improved method for the estimation of surface roughness of obstacle arrays. Atmos. Environ. 32, 1857–1864. Available from: https://doi.org/10.1016/S1352-2310(97)00403-2.

Nakamura, Y., Oke, T.R., 1988. Wind, temperature and stability conditions in an east-west oriented urban canyon. Atmos. Environ. 22, 2691–2700. Available from: https://doi.org/10.1016/0004-6981(88)90437-4.

Stockie, J.M., 2011. The mathematics of atmospheric dispersion modeling. SIAM Rev. 53, 349–372. Available from: https://doi.org/10.1137/10080991X.

Venkatram, A., Isakov, V., Thoma, E., Baldauf, R., 2007. Analysis of air quality data near roadways using a dispersion model. Atmos. Environ. 41, 9481–9497. Available from: https://doi.org/10.1016/j.atmosenv.2007.08.045.